A Velocity Independent Pressure Drag for Sub-Critical Two-Layer Shallow-Water Flow Around an Inclined Oceanic Ridge : a Numerical Study

Achim Wirth
achim.wirth@legi.cnrs.fr

Abstract: We present results from numerical simulations which show that the pressure drag of a sub-critical two-layer shallow-water flow, in a rotating frame, around an inclined ridge is almost independent of the fluid speed for a large range of Rossby numbers. This behavior is observed for barotropic and baroclinic flows approaching the ridge. This result is a counter example to what is actually believed in geophysical fluid dynamics and employed in parameterizations of topographic effects, which are commonly based on a quadratic drag law. The behavior is explained by the observation that for larger fluid speeds the fluid crosses the ridge at lower depth leading to a shorter path-length. As the frictional head loss is a product of the velocity and the path length, both compensate.

Ridges and Pressure Drag

In 1786 Du Buat measured the pressure over the surface of an obstacle in a moving fluid. He observed, that the pressure at the up-flow side exceeds the pressure at the down-flow side. This pressure difference leads to a pressure drag.

The most prominent physical process considered to discuss oceanic-flow and topography interaction is the Antarctic Circumpolar Current (ACC) and the Reykjanes Ridge but also smaller scale features as dynamics around ridges in a tidal channel are considered. Recently, the atmospheric flow patterns around a ridge have been investigated to explain the increase of the summer near-surface temperatures over the northeast coast of the Antarctic Peninsula. Results from numerical and laboratory experiments suggests that a change from blocked flow around the ridge to flow over the ridge can explain the anomaly strong local warming.

When in fluid dynamics the dependence of the drag on the fluid velocity is considered in analytical calculations or parameterizations of pressure drag the prominent quadratic-drag law is almost always employed. The law is based on the simple fact the inertia is the product of mass and velocity and that the mass of fluid encountering an obstacle is itself a linear function of velocity. The law applies also to the frictional forces in a turbulent boundary layer. A large amount of research in all fields of fluid dynamics is dedicated to determining the friction coefficient, taking the quadratic law for granted. There are however instances where the drag escapes the quadratic law and shows a different behavior. An interesting example is the drag of flexible objects (plants) in flow, as membrane configurations for which the drag force is almost independent of fluid speed, when it is within a certain range. Other examples of velocity independent drag are low Reynolds number flow of DNA molecules and objects moving within a granular medium. In our work we will show that the the pressure drag of a two-layer oceanic flow in a rotating frame that encounters an inclined ridge is another example.

Experiments

Bottom topography

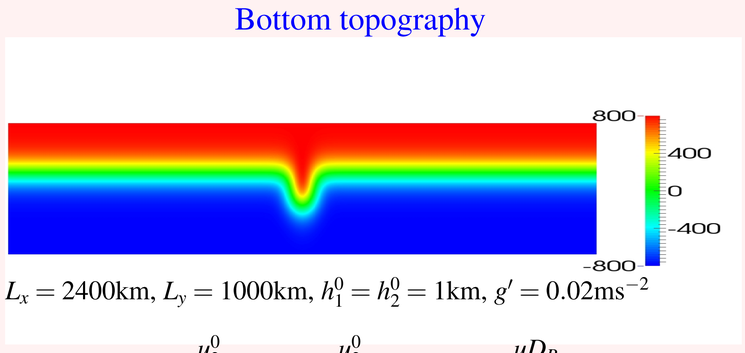

$L_x = 2400\text{km}$, $L_y = 1000\text{km}$, $h_1^0 = h_2^0 = 1\text{km}$, $g' = 0.02\text{ms}^{-2}$

$$\varepsilon = \frac{u_2^0}{D_R f},\ Fr = \frac{u_2^0}{\sqrt{g' h_e^0}} < 1,\ Re = \frac{u D_R}{\nu}$$

2 layer Shallow Water Equations

$$\begin{aligned}
\partial_t u_1 + & \quad u_1\partial_x u_1 + v_1\partial_y u_1 + g\partial_x \eta_1 - f v_1 = \nu\nabla^2 u_1 \\
\partial_t v_1 + & \quad u_1\partial_x v_1 + v_1\partial_y v_1 + g\partial_y \eta_1 + f u_1 = \nu\nabla^2 v_1 \\
\partial_t \eta_1 + & \ \partial_x[h_1 u_1] + \partial_y[h_1 v_1] + \partial_x[h_2 u_2] + \partial_y[h_2 v_2] = \kappa\nabla^2 \eta_1 \\
\partial_t u_2 + & \ u_2\partial_x u_2 + v_2\partial_y u_2 + g''\partial_x \eta_1 + g'\partial_x \eta_2 - f v_2 = \nu\nabla^2 u_2 \\
\partial_t v_2 + & \ u_2\partial_x v_2 + v_2\partial_y v_2 + g''\partial_y \eta_1 + g'\partial_y \eta_2 + f u_2 = \nu\nabla^2 v_2 \\
\partial_t \eta_2 + & \quad \partial_x[h_2 u_2] + \partial_y[h_2 v_2)] = \kappa\nabla^2 \eta_2
\end{aligned}$$

exp	l1	l2	f (10^{-4})	ν	ε	Re
e001	0.1	0.1	1.	100.	0.016	40
e002	0.25	.25	1.	100.	0.04	100
e003	0.5	0.5	1.	100.	0.08	200
e004	0.75	.75	1.	100.	0.12	300
e005	1.0	1.0	1.	100.	0.16	400
e006	1.5	1.5	1.	100.	0.24	600
e007	2.0	2.0	1.	100.	0.32	800
e012	0.25	.25	1.	200.	0.04	50
e013	0.5	0.5	1.	200.	0.08	100
e015	1.0	1.0	1.	200.	0.16	200
e017	2.0	2.0	1.	200.	0.32	400
e025	1.0	1.0	1.	50.	0.16	800
e105	1.0	1.0	2.	100.	0.08	400
e205	1.0	1.0	3.	100.	0.0533	400
e305	1.0	1.0	4.	100.	0.04	400
e1001	0.1	0.1 λ	1.	100.	0.032	80
e1002	0.1	0.25 λ	1.	100.	0.056	140
e1003	0.1	0.5 λ	1.	100.	0.096	240
e1005	0.1	1.0 λ	1.	100.	0.176	440
e1006	0.1	1.05 λ	1.	100.	0.184	480

Results: Inertial Dynamics

exp005

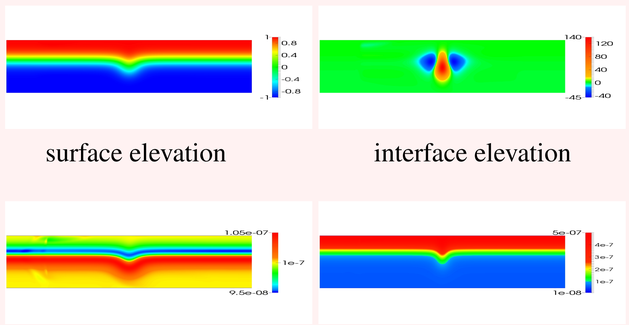

Strong fore-aft symmetry, almost time independent (faint trapped Poincaré waves).

The flow is almost time independent (faint trapped Poincaré waves above topography). The dynamics is governed by the conservation of potential vorticity (PV) in each layer: $\vec{u}_i \cdot \nabla q_i = 0$ with $q_i = \frac{\zeta_i + f}{h_i}$. And the Bernoulli potential assures the symmetry of stationary flow across a symmetric ridge. For the low velocity case the Rossby number is small, that is the relative vorticity is small as compared to the Coriolis parameter and the flow flows around the topography in the lower layer. For higher velocities the relative vorticity becomes more important, it is negative at the tip of the topography. To compensate the reduction of total vorticity $(\zeta_i + f)$ the layer thickness decreases as the flow crosses the ridge further above the topography. This leads, at the same time, to a decrease of the relative vorticity as the flow performs a less pronounced bend around the topography. This is clearly visible in Fig. to the right where the path of the center of the current around the ridge in the two layers for different Rossby number is shown.

Current Paths

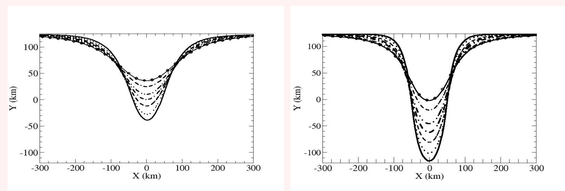

upper layer lower layer

Paths of the center of the current in the upper layer (left) and the lower layer (right) for ex001 (—), ex002 ($\cdots$), ex003 ($- - -$), ex004 ($\cdot - \cdot$), ex005 ($- \cdots -$), ex006 ($\cdot - - \cdot$), ex007 (-⊖-)

Results : Dissipative Processes

Pressure Drag

$$\begin{aligned}
D_b &= g\int_A (\rho_1 h_1 + \rho_2 h_2)\partial_x b\, da \\
&= D_{b1} + D_{b2}
\end{aligned}$$

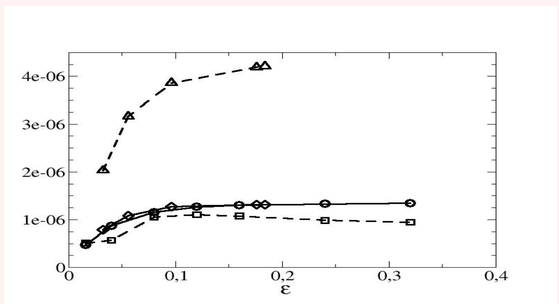

Pressure drag as a function of the Rossby number (ε). Total pressure drag of exp00X (○) and exp10X (◇) and pressure drag due to the interface for exp00X () and exp10X (△).

When considering the path of the flow around the ridge we can observe a slight asymmetry across the ridge, which is proportional to viscosity. It is a measure of the frictional head-loss across the ridge and is almost proportional to the viscosity value, the velocity (linear friction) and the path length. As we have seen in the previous section that stronger flow leads to a shorter path length and so when considering the friction as a function of the Rossby number we find the pressure drag is, in the case considered here, almost independent of it.

For the experiments with a baroclinic forcing the total pressure drag is almost identical to the barotropic forcing when plotted as a function of the Rossby number in the lower layer as shown in the Fig. The pressure drag due to the interface is however five-fold higher but it is then compensated by a negative pressure drag due to the surface.

Perspectives

The behavior is remarkably robust law as results with a baroclinicly forced flow lead to almost identical results for the total pressure drag. This and the fact that the findings are explained by the conservation of potential vorticity suggest that our results are more than a curiosity in geophysical fluid dynamics.

Although the configuration is highly idealized we did not find analytical solutions and the results are numerical. The presence of very low amplitude trapped Poincaré waves indicates that these solutions are probably not readily available. This is common to the field flow topography interaction were analytical solutions are scant even in the most idealized cases.

We further like to mention that the width of the ridge (50km) is smaller than the grid-size of most numerical models used to simulate the ocean dynamics in climate models. The influence of such a ridge has therefore to be parameterized and the present work questions the validity of the available parameterizations, which are based on a quadratic law.